Since January 2020 Elsevier has created a COVID-19 resource centre with free information in English and Mandarin on the novel coronavirus COVID-19. The COVID-19 resource centre is hosted on Elsevier Connect, the company's public news and information website.

Science of the Total Environment 839 (2022) 156164

Contents lists available at ScienceDirect

Science of the Total Environment

journal homepage: www.elsevier.com/locate/scitotenv

A new-type HOCl-activatable fluorescent probe and its applications in water environment and biosystems

Kun Wang [a], Yilin Liu [a], Caiyun Liu [a,*], Hanchuang Zhu [a], Xiwei Li [a], Miaohui Yu [b], Lunying Liu [a], Guoqing Sang [a], Wenlong Sheng [b,*], Baocun Zhu [a,*]

[a] School of Water Conservancy and Environment, University of Jinan, Jinan 250022, China
[b] Biology Institute, Qilu University of Technology (Shandong Academy of Sciences), Jinan 250103, China

HIGHLIGHTS

- The probe showed rapid response (within seconds) to HOCl with high selectivity.
- The probe could quantitatively detect HOCl with high sensitivity, and the limit of detection was 17 nM.
- The probe could be used to detect HOCl in actual water samples.
- The probe could realize the precision discrimination between normal cells and cancer cells.

GRAPHICAL ABSTRACT

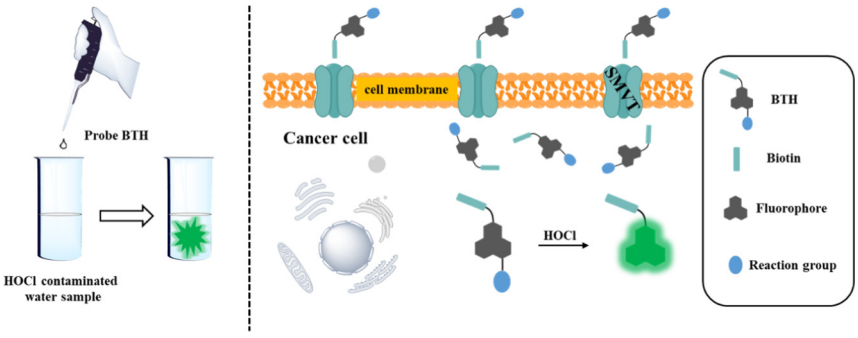

ARTICLE INFO

Editor: Damià Barcelò

Keywords:
Biotin
Cancer cells
Fluorescent probe
Hypochlorous acid
Water samples

ABSTRACT

The outbreak and spread of Corona Virus Disease 2019 (COVID-19) has led to a significant increase in the consumption of sodium hypochlorite (NaOCl) disinfectants. NaOCl hydrolyzes to produce hypochlorous acid (HOCl) to kill viruses, which is a relatively efficient chlorine-based disinfectant commonly used in public disinfection. While people enjoy the convenience of NaOCl disinfection, excessive and indiscriminate use of it will affect the water environment and threaten human health. Importantly, HOCl is an indispensable reactive oxygen species (ROS) in human body. Whether its concentration is normal or not is closely related to human health. Excessive production of HOCl in the body contributes to some inflammatory diseases and even cancer. Also, we noticed that the concentration of ROS in cancer cells is about 10 times higher than that in normal cells. Herein, we developed a HOCl-activatable biotinylated dual-function fluorescent probe BTH. For this probe, we introduced biotin on the naphthalimide fluorophore, which increased the water solubility and enabled the probe to aggregate in cancer cells by targeting specific receptor overexpressed on the surface of cancer cell membrane. After reacting to HOCl, the *p*-aminophenylether moiety of this probe was oxidatively removed and the fluorescence of the probe was recovered. As expected, in the PBS solution with pH of 7.4, BTH could give full play to the performance of detecting HOCl, and it has made achievements in detecting the concentration of HOCl in actual water samples. Besides that, BTH had effectively distinguished between cancer cells and normal cells through a dual-function discrimination strategy, which used biotin to enrich the probe in cancer cells and reacted with overexpressed HOCl in cancer cells. Importantly, this dual-function discrimination strategy could obtain the precision detection of cancer cells, thereby offering assistance for improving the accuracy of early cancer diagnosis.

* Corresponding authors.
E-mail addresses: liucaiyun1982072@163.com (C. Liu), 15618694162@163.com (W. Sheng), lcyzbc@163.com (B. Zhu).

http://dx.doi.org/10.1016/j.scitotenv.2022.156164
Received 14 February 2022; Received in revised form 18 May 2022; Accepted 19 May 2022
Available online 21 May 2022

1. Introduction

Since the outbreak of Corona Virus Disease 2019 (COVID-19) began, there have been serious consequences (Chen et al., 2021; WHO, 2021). Countries attach great importance to disinfection and sterilization in public places because of the seriousness of the epidemic (Lewis, 2021; Service, 2020). Sodium hypochlorite (NaOCl) solution is a chlorine-based disinfectant whose active ingredient is sodium hypochlorite, which can be hydrolyzed into hypochlorous acid (HOCl) and then produce disinfection and sterilization effect. NaOCl is also listed by the U.S. Environmental Protection Agency as one of the most used disinfection active ingredients to contain COVID-19 (EPA, 2021). On the bright side, the use of NaOCl disinfectant has contributed to limiting the spread of the outbreak. However, incorrect and indiscriminate use of disinfectants containing NaOCl will increase the potential risk of ecological and environmental damage (Chen et al., 2021; Nabi et al., 2020; Thakur et al., 2021). Recent reports indicate that the residues of NaOCl disinfectant entering water will pollute it, posing a threat to aquatic life, causing ecological damage, and then affecting human health (Chu et al., 2020; Rafiee et al., 2022; Zhang et al., 2020). Therefore, it is a significant topic to detect whether there is excessive HOCl in water environment.

On the other hand, HOCl is a vital small molecule in organisms, belonging to one of the reactive oxygen species (ROS), produced by the action of myeloperoxidase (MPO) on chloride ions (Cl^-) and hydrogen peroxide (H_2O_2), and plays a pivotal role in cell signaling and immune defense system (He et al., 2020; B. Wang et al., 2021; Xu et al., 2013; Rayner et al., 2018; Bauer, 2018). As a "double-edged sword", HOCl has an evil side. It has been reported that some inflammatory diseases and even cancer are related to excessive HOCl concentration (Duan et al., 2019; Hou et al., 2022; Zhu et al., 2018; Pan et al., 2012). Significantly, the concentration of ROS in cancer cells is about 10 times higher than that in normal cells (Antunes and Cadenas, 2001; L. Wang et al., 2021; Ye et al., 2017), which may assist in distinguishing between cancer cells and normal cells. Thus, tracing HOCl in biosystems is also of extraordinary significance.

Compared with traditional methods, small molecule fluorescent probes have attracted additional attention in virtue of their advantages including non-invasiveness, simple operation and real-time imaging (S. Wang et al., 2021; Shu et al., 2020; L. Wu et al., 2021; X. Wu et al., 2021; Rong et al., 2021; Zhu et al., 2016). The currently reported HOCl fluorescent probes have relatively simple functions, and have some disadvantages such as low sensitivity, long response time and poor water solubility. (Gao et al., 2021; Hou et al., 2020; Li et al., 2017; Zhu et al., 2021; Zhu et al., 2014). With regards to this, we designed and synthesized a HOCl-activatable biotinylated fluorescent probe BTH to improve the above shortcomings (Scheme 1).

As a result of the introduction of the biotin functional group, the water solubility of BTH is increased, which provides a favorable condition for the detection of HOCl in aqueous solution. More importantly, biotin is a pivotal cofactor of carboxylase activity, and it is more favored by rapidly proliferating cells especially cancer cells (Jang et al., 2017; Said, 1999; Yang et al., 2009). It is reported that the sodium-dependent multivitamin transporter (SMVT) is overexpressed on the membrane surface of cancer cells to ensure the uptake of biotin by cells (Błauż et al., 2021; Maiti et al., 2013; Vadlapudi et al., 2012). Hence, BTH containing biotin is more likely to be enriched in cancer cells, which is instrumental in avoiding the "false positive" results when distinguishing between normal cells and cancer cells (She et al., 2021; Wang and Chen, 2021). On the other side, we modified naphthimide fluorophore with *p*-aminophenylether an excellent reaction group of HOCl. BTH was non-fluorescent, which was ascribed to the photo-induced electron transfer (PET) effect produced by this reactive group (Jia et al., 2019). As expected, in the PBS solution with pH of 7.4, the probe BTH showed high sensitivity (LOD = 17 nM), rapid response and specific fluorescence turn-on in the presence of HOCl, and BTH could be applied to the detection of HOCl in actual water samples. It was worth mentioning that BTH successfully discriminated between normal cells and cancer cells by the way of this dual-function discrimination strategy that utilize the enrichment effect of biotin and the excessive concentration of HOCl, and it could become a useful tool for early cancer diagnosis.

2. Experimental section

The specific details of chemicals, instruments, and experimental operations can be found in the supporting information. The synthetic route of BTH is shown in Scheme 1, and the synthesis of intermediate compounds is also provided.

2.1. Synthesis of probe BTH

Compound 3 (347 mg, 1 mmol) was dissolved in anhydrous dichloromethane (DCM) (10 mL). A solution of D-Biotin (488 mg, 2 mmol) and 4-dimethylaminopyridine (DMAP) (244 mg, 2 mmol) in anhydrous *N*,*N*-dimethylformamide (DMF) (10 mL) was then added. Subsequently, dicyclohexylcarbodiimide (DCC) (412 mg, 2 mmol) was added in the above mixed solution. The reaction was stirred at room temperature for 16 h. Then, the DCM from the solution was removed by vacuum concentration. After adding 150 mL of distilled water to the remaining solution, the solid was separated out. The crude product was purified by column chromatography over silica gel (dichloromethane: methanol = 30: 1, v/v, as eluent) to afford probe BTH. ^{1}H NMR (400 MHz, DMSO-d_6) δ (ppm): 8.685 (d, J = 7.2 Hz, 1H), 8.516 (d, J = 5.6 Hz, 1H), 8.345 (d, J = 7.2 Hz, 1H), 7.905–7.849 (m, 2H), 6.976 (d, J = 6.8 Hz, 2H), 6.848 (d, J = 7.6 Hz, 1H), 6.708 (d, J = 6.8 Hz, 2H), 6.412 (d, J = 20.0 Hz, 2H), 5.232 (s, 2H), 4.307–4.066 (m, 4H), 2.798 (d, J = 11.6 Hz, 1H), 2.570 (d, J = 12.4 Hz, 2H), 1.939 (s, 2H), 1.523–1.177 (m, 6H). ^{13}C NMR (100 MHz, DMSO-d_6) δ (ppm): 172.69, 164.20, 163.51, 163.16, 161.07, 147.32, 144.12, 133.25, 131.70, 129.48, 128.60, 127.16, 123.28, 122.66, 122.12, 115.71, 115.47, 109.67, 61.42, 59.65, 55.81, 36.83, 35.71, 28.54, 28.42, 25.60. HRMS (ESI): Calcd for $C_{30}H_{32}N_5O_5S$ $[M + H]^+$ 574.2119; Found, 574.2118.

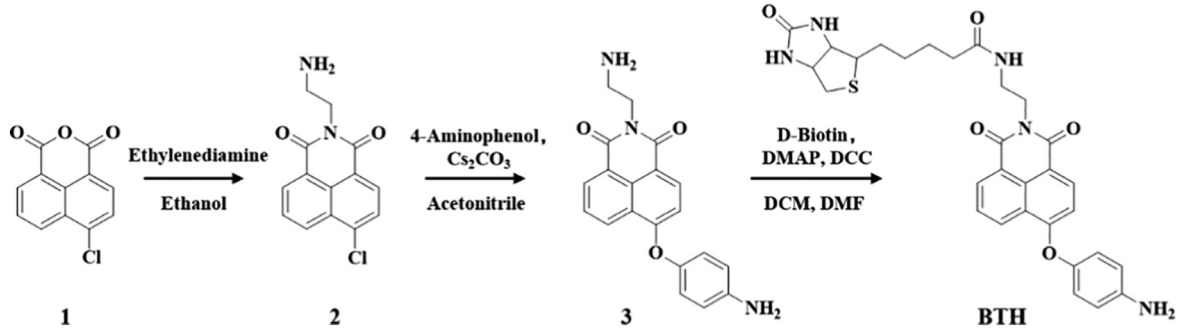

Scheme 1. The synthetic route of **BTH**.

3. Results and discussion

3.1. Rational design and recognition mechanism of BTH

BTH was constructed on the 4-hydroxy-1,8-naphthalimide fluorophore reported firstly by our group (Zhu et al., 2011). This fluorophore had a conspicuous intramolecular charge transfer (ICT) structure, which had aroused widespread concern (Park et al., 2020; Wen et al., 2017; Zhou et al., 2019). Furthermore, the *p*-aminophenylether receptor had been reported to be a good HOCl detection group and it could produce the PET effect to hinder the luminescence of BTH (Jia et al., 2019). After BTH reacted with HOCl, the fluorescence was turned on. Thus, we bonded 4-aminophenol to the fluorophore by a nucleophilic substitution reaction to form ether bond like compound 3. The carboxylic acid moiety on biotin was connected to the naphthalimide framework through an amide bond, which could increase the water solubility of BTH and its ability to aggregate in cancer cells (Jung et al., 2014). Then, we characterized the structure of BTH by ^{1}H NMR and ^{13}C NMR, and the product of the reaction of BTH and HOCl was confirmed by HRMS. The proposed reaction mechanism was that the *p*-aminophenylether part of the probe was removed by HOCl oxidation (Scheme 2).

3.2. Time-dependent experiment of BTH towards HOCl

After verifying the correct structure of BTH by means of characterization, a series of sensing properties of BTH for responding HOCl were discussed, using the aqueous solution as test solution with the addition of phosphate buffered saline (PBS) solution (pH = 7.4). To start with, the time kinetics experiment of BTH response to HOCl was studied. As could be seen from Fig. 1, adding HOCl (5 μM) to the probe (5 μM) solution (10 mM PBS, pH = 7.4), the reaction could be completed within a few seconds. The fluorescence intensity at 553 nm reached the maximum and remained unchanged. This ability of BTH to react rapidly to HOCl, benefiting from *p*-aminophenylether group, suggested that BTH could detect HOCl quickly in aqueous solution and had the potential to capture HOCl in biological systems.

3.3. Quantitative test of HOCl

Furthermore, we performed a fluorescence titration experiment with HOCl from 0 to 30 μM in the PBS solution of BTH (5 μM). As shown in Fig. 2A, BTH was barely provided with luminescent properties, which was ascribed to the PET effect produced by the *p*-aminophenylether receptor. After adding HOCl with a concentration of 0 to 30 μM to the PBS solution of BTH, a significant emission peak at 553 nm was observed and the fluorescence intensity increased gradually. In the meanwhile, when HOCl was in the low concentration range from 0 to 1 μM, there existed a good linear correlation that the Y-axis represented the fluorescence intensity at 553 nm, and the X-axis represented the concentration of HOCl (Fig. 2B). The linear regression equation was got as y = 102,923 × [HOCl] (μM) + 35,601 and the square of the correlation coefficient was 0.9965. The limit of detection was calculated as low as 17 nM. This result indicated that BTH can be used to detect HOCl in aqueous solution and will be a potential tool for detecting HOCl in actual water samples. It was sufficiently sensitive to HOCl under simulated physiological conditions and was conducive to tracing it in biosystems.

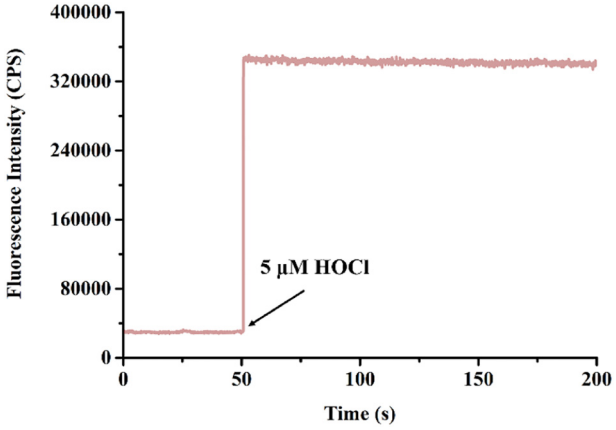

Fig. 1. Time kinetic spectra of probe BTH (5 μM) response to HOCl (5 μM) under the PBS solution (10 mM, pH 7.4) at 25 °C. λ_{ex} = 468 nm.

3.4. Selectivity of BTH for HOCl

Subsequently, we evaluated the responsiveness of BTH to various analytes including ions, biological mercaptans and other reactive oxygen species (Fig. 3). The fluorescence of BTH at 553 nm did not change significantly when other higher concentrations of analytes were added. On the contrary, low concentrations of HOCl could cause strong fluorescence enhancement. In other words, BTH showed satisfactory selectivity to HOCl. Overall, it was implied that BTH was feasible in the discrimination of HOCl in aqueous solution.

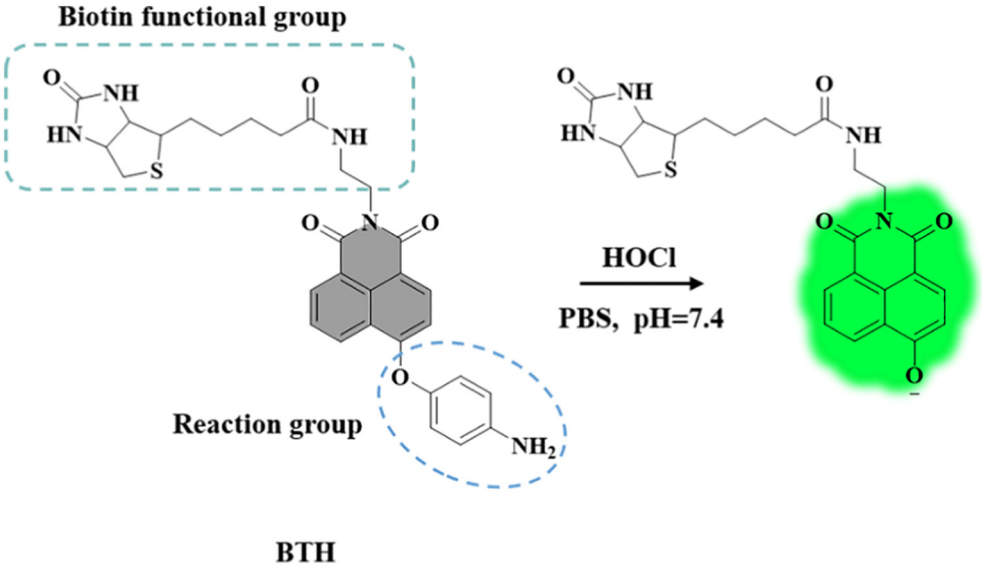

Scheme 2. The proposed response mechanism of **BTH**.

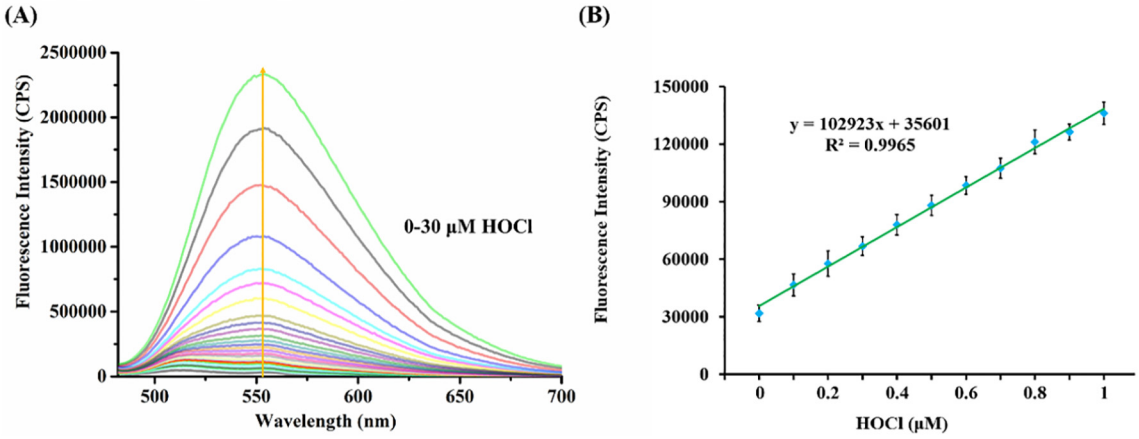

Fig. 2. (A) Fluorescence spectra changes of probe BTH (5 μM) before and after adding HOCl (0–30 μM) under the PBS solution (10 mM, pH 7.4) at 25 °C. (B) The relationship between the fluorescence intensity at 553 nm of BTH (5 μM) and the concentration of added HOCl (0–1 μM). λ_{ex} = 468 nm.

3.5. Analytical applications of BTH in water samples

Since high concentrations of HOCl in water can cause water pollution and the death of aquatic organisms, it is of great significance to detect hypochlorous acid in the water environment. Considering the above reasons, as well as the results of the spectral test, we were motivated to apply BTH to the detection of HOCl in practical water samples (Table 1). Three water samples were collected in this work. First, the large impurities in the water sample were filtered out, and then the treated water sample was analyzed with BTH. The results show that no HOCl at a higher concentration than 17 nM could be detected in the three water samples. Next, 0.5 μM and 1 μM HOCl were added to the treated water samples and recovered. The three water samples in the experiment have good recoveries with 93.13%–107.83%. It indicated that BTH could be applied to detecting HOCl in actual water samples.

3.6. Fluorescence imaging applications of BTH in live cells

The cytotoxicity of BTH was first evaluated before the ability to apply it in living cells. As shown in Fig. S1, the results of cell counting kit (CCK-8) analysis showed that BTH had low toxicity to HeLa cells. After that, we studied the ability of BTH to trace endogenous and exogenous HOCl in HeLa cells by confocal microscopy (Fig. 4). The cells (Fig. 4b) incubated with only BTH showed stronger green fluorescence than the control cells (Fig. 4a). Then, HOCl (10 μM) was added to the group b and the green fluorescence was more obvious (Fig. 4c). Equally, the cells that were stimulated with LPS (Lipopolysaccharide, an inflammatory stimulant) and then treated with BTH displayed intense fluorescence (Fig. 4d). On the contrary, the fluorescence of the cells which were pretreated with NAC (Nacetyl-L-cysteine, a hypochlorite scavenger) and then incubated with BTH was feeble (Fig. 4e). Fig. 4f had compared the fluorescence intensity of cells in each group. These imaging data demonstrated that BTH could be used to trace intracellular HOCl.

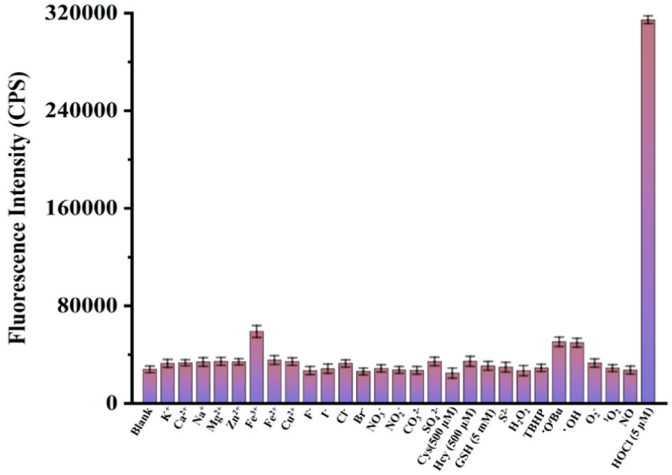

Fig. 3. The fluorescence intensity at 553 nm of probe BTH (5 μM) to analytes (except for the marked concentration, the others are 100 μM) under the PBS solution (10 mM, pH 7.4) at 25 °C. λ_{ex} = 468 nm.

3.7. Application of BTH in distinguishing normal cells and cancer cells

Considering the design idea of BTH, in order to verify the ability of it to distinguish between normal cells and cancer cells, we selected two types of normal cells (RAW 264.7 and HUVEC cells) and four types of cancer cells (MGC-803, HeLa, HepG2 and SH-SY5Y cells) for the experiment. The above six kinds of cells were incubated with BTH for 25 min. As expected, the RAW 264.7 and HUVEC cells showed weak fluorescence (Fig. 5a). In contrast, the green fluorescence of the MGC-803, HeLa, HepG2 and SH-SY5Y cells was especially strong (Fig. 5b). The histogram also showed a big difference in the fluorescence intensity between normal cells and cancer cells (Fig. 5c). It could be said that BTH had potential application in differentiating between normal cells and cancer cells.

Subsequently, another experiment demonstrated that the biotin portion of BTH could enable BTH to be enriched in cancer cells. We selected HeLa cells for biotin inhibition experiment. Cells incubated with biotin followed by BTH (Fig. 6c) showed weaker fluorescence intensity than cells incubated with BTH only (Fig. 6b). The histogram was more intuitive (Fig. 6d). This result could be ascribed to the early incubation of biotin occupying the receptor channel on the cell surface and thus blocking the uptake of BTH (Chai et al., 2021).

On the other hand, we performed the same discrimination experiment using probe BAH, a probe not modified with biotin (Jia et al., 2019).

Table 1
Performance of BTH in three actual water samples (Sample A: Tap Water, University of Jinan; Sample B: Jia Zi Lake, University of Jinan; Sample C: Wohushan reservoir in Jinan, China).

Water samples	Found HOCl	Added/μM	Found/μM (n = 3)	Recovery/%
Sample A	ND	0.5	0.49 ± 0.13	97.21
		1	1.06 ± 0.07	105.61
Sample B	ND	0.5	0.47 ± 0.15	93.13
		1	0.98 ± 0.14	97.69
Sample C	ND	0.5	0.54 ± 0.03	107.83
		1	1.05 ± 0.04	105.42

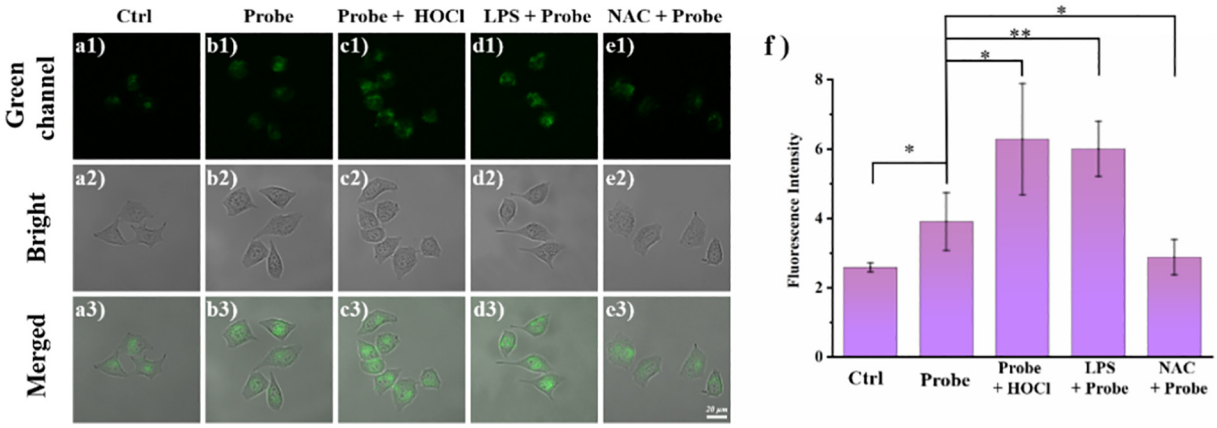

Fig. 4. Fluorescence imaging of probe BTH in HeLa cells. a) Control cells; b) Cells treated with BTH; c) Cells in group b treated with HOCl (10 μM); d) Cells pretreated with LPS (Lipopolysaccharide, an inflammatory stimulant, 1.0 μg mL^{-1}) for 12 h and then incubated with BTH (10 μM); e) Cells pretreated with NAC (Nacetyl-L-cysteine, a hypochlorite scavenger, 500 μM) for 2 h and then treated with BTH (10 μM); f) Fluorescence intensity statistics graph of each group of cells. The time of treating cells with BTH (10 μM) and HOCl (10 μM) is both 25 min. All cells were treated at 37 °C. λ_{ex} = 472 nm, λ_{em} = 485–585 nm.

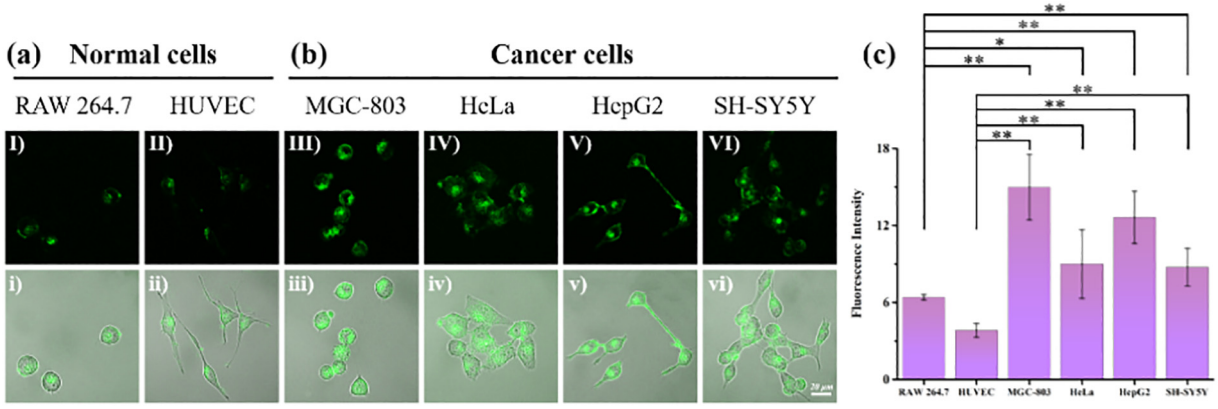

Fig. 5. The application of probe BTH to distinguish between normal cells and cancer cells. (a) Normal cells incubated with BTH (10 μM) for 25 min at 37 °C, (I-i) RAW 264.7 cells, (II-ii) HUVEC; (b) Cancer cells incubated with BTH (10 μM), for 25 min at 37 °C, (III-iii) MGC-803, (IV-iv) HeLa, (V-v) HepG2, (VI-vi) SH-SY5Y; (c) Fluorescence intensity statistics graph of six kinds of cells. The cells were treated with BTH (10 μM) for 25 min at 37 °C. λ_{ex} = 472 nm, λ_{em} = 485–585 nm.

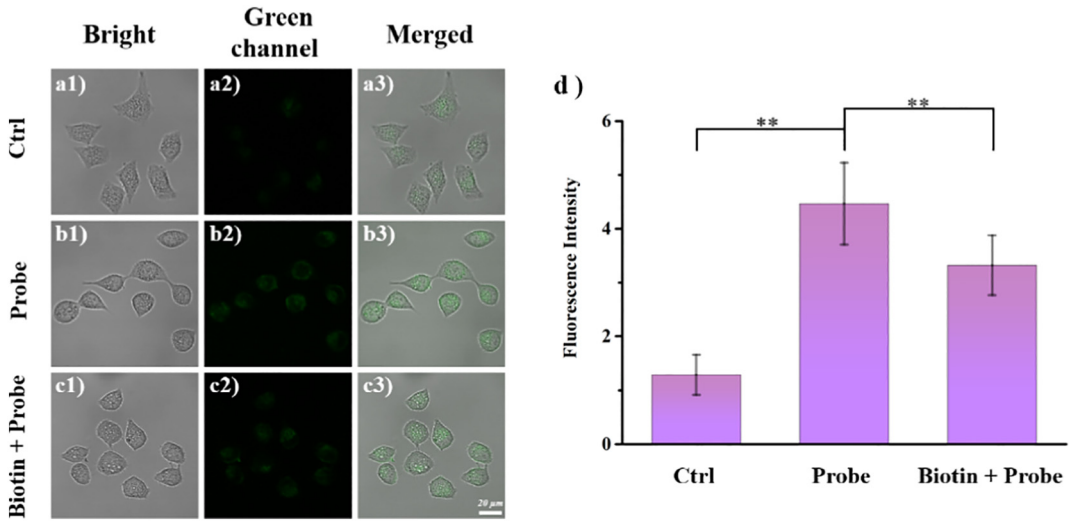

Fig. 6. Fluorescence imaging of biotin inhibition experiment. a) Control cells; b) Cells incubated with probe BTH (10 μM); c) Cells pretreated with biotin (50 μM) and then treated with probe BTH (10 μM); d) Fluorescence intensity statistics graph of each group of cells. The cells were treated with probe BTH (10 μM) for 25 min or biotin (50 μM) for 30 min at 37 °C. λ_{ex} = 472 nm, λ_{em} = 485–585 nm.

BAH, without the assistance of biotin, did not tend to accumulate in cancer cells. The fluorescence of the six kinds of cells was closely after incubation with BAH (Fig. S9), so the control probe was going to confuse cancer cells with normal cells. These above results might provide forceful evidence that BTH could be a useful tool for tumor imaging.

4. Conclusions

In this work, we designed and synthesized a biotin-functionalized fluorescent probe BTH. When there existed HOCl, BTH with good water solubility and high sensitivity could selectively turn on fluorescence as well as had the ability of rapid respond, which could be used for the detection of HOCl in aqueous solution. Moreover, the biotin part of BTH could enrich it in cancer cells, and with the help of the difference in the basal HOCl concentration between normal cells and cancer cells, that could avoid "false positive" results and achieved the purpose of effectively distinguishing normal cells and cancer cells. Hence, we do hope that BTH might be a useful tool for detecting excessive HOCl in water environment and the early diagnosis of cancer.

CRediT authorship contribution statement

Kun Wang: Investigation, Data curation, Writing - original draft.
Yilin Liu: Investigation, Data curation.
Caiyun Liu: Conceptualization, Review & Editing.
Hanchuang Zhu: Formal analysis.
Xiwei Li: Formal analysis.
Miaohui Yu: Investigation, Data curation.
Lunying Liu: Investigation, Data curation.
Guoqing Sang: Investigation, Data curation.
Wenlong Sheng: Data curation, Writing - Review & Editing.
Baocun Zhu: Project administration.

Declaration of Competing Interest

The authors declare that they have no known competing financial interests or personal relationships that could have appeared to influence the work reported in this paper.

Acknowledgements

We gratefully acknowledge financial support from the NSFC (22176070 and 21777053), A Project of Shandong Province Higher Educational Youth Innovation Science and Technology Program (2019KJD005), and the Open Research Fund of State Key Laboratory of Simulation and Regulation of Water Cycle in River Basin, China Institute of Water Resources and Hydropower Research (IWHR-SKL-201519).

Appendix A. Supplementary data

Supplementary data to this article can be found online at https://doi.org/10.1016/j.scitotenv.2022.156164.

References

Antunes, F., Cadenas, E., 2001. Cellular titration of apoptosis with steady-state concentrations of H2O2: submicromolar levels of H2O2 induce apoptosis through Fenton chemistry independent of the cellular thiol state. Free Radic. Biol. Med. 30, 1008–1018. https://doi.org/10.1016/S0891-5849(01)00493-2.

Bauer, G., 2018. HOCl and the control of oncogenesis. J. Inorg. Biochem. 179, 10–23. https://doi.org/10.1016/j.jinorgbio.2017.11.005.

Błauż, A., Rychlik, B., Plazuk, D., Peccati, F., Jiménez-Osés, G., Steinke, U., Sierant, M., Trzeciak, K., Skorupskad, E., Miksa, B., 2021. Biotin-phenosafranin as a new photosensitive conjugate for targeted therapy and imaging. New J. Chem. 45, 9691–9702. https://doi.org/10.1039/D0NJ06170K.

Chen, B., Han, J., Dai, H., Jia, P., 2021. Biocide-tolerance and antibiotic-resistance in community environments and risk of direct transfers to humans: unintended consequences of community-wide surface disinfecting during COVID-19?*. Environ. Pollut. 283, 117074. https://doi.org/10.1016/j.envpol.2021.117074.

Chu, W., Fang, C., Deng, Y., Xu, Z., 2020. Intensified disinfection amid COVID-19 pandemic poses potential risks to water quality and safety. Environ. Sci. Technol. 55, 4084–4086. https://doi.org/10.1021/acs.est.0c04394.

Chai, Z., Liu, D., Li, X., Zhao, Y., Shi, W., Li, X., Ma, H., 2021. A tumor-targeted near-infrared fluorescent probe for HNO and its application to the real-time monitoring of HNO release in vivo. Chem. Commun. 57, 5063–5066. https://doi.org/10.1039/D1CC01462E.

Duan, Q., Jia, P., Zhuang, Z., Liu, C., Zhang, X., Wang, Z., Sheng, W., Li, Z., Zhu, H., Zhu, B., Zhang, X., 2019. Rational design of a hepatoma-specific fluorescent probe for HOCl and its bioimaging applications in living HepG2 cells. Anal. Chem. 91, 2163–2168. https://doi.org/10.1021/acs.analchem.8b04726.

EPA, 2021. List N Advanced Search Page: Disinfectants for Coronavirus (COVID-19). https://www.epa.gov/pesticide-registration/list-n-advanced-search-page-disinfectants-coronavirus-covid-19.

Gao, W., Ma, Y., Liu, Y., Ma, S., Lin, W., 2021. Observation of endogenous HClO in living mice with inflammation, tissue injury and bacterial infection by a near-infrared fluorescent probe. Sens. Actuators B Chem. 327, 128884. https://doi.org/10.1016/j.snb.2020.128884.

He, X., Chen, H., Xu, C., Fan, J., Xu, W., Li, Y., Deng, H., Shen, J., 2020. Ratiometric and colorimetric fluorescent probe for hypochlorite monitor and application for bioimaging in living cells, bacteria and zebrafish. J. Hazard. Mater. 388, 122029. https://doi.org/10.1016/j.jhazmat.2020.122029.

Hou, J.-T., Kwon, N., Wang, S., Wang, B., He, X., Yoon, J., Shen, J., 2022. Sulfur-based fluorescent probes for HOCl: mechanisms, design, and applications. Coordin. Chem. Rev. 450, 214232. https://doi.org/10.1016/j.ccr.2021.214232.

Hou, J.-T., Wang, B., Zou, Y., Fan, P., Chang, X., Cao, X., Wang, S., Yu, F., 2020. Molecular fluorescent probes for imaging and evaluation of hypochlorite fluctuations during diagnosis and therapy of osteoarthritis in cells and in a mouse model. ACS Sens. 5, 1949–1958. https://doi.org/10.1021/acssensors.0c00270.

Jia, P., Zhuang, Z., Liu, C., Wang, Z., Duan, Q., Li, Z., Zhu, H., Du, B., Zhu, B., Sheng, W., Kang, B., 2019. A highly specific and ultrasensitive p-aminophenylether-based fluorescent probe for imaging native HOCl in live cells and zebrafish. Anal. Chim. Acta 1052, 131–136. https://doi.org/10.1016/j.aca.2018.11.031.

Jang, J.H., Kim, W.R., Sharma, A., Cho, S.H., James, T.D., Kang, C., Kim, J.S., 2017. Targeted tumor detection: guidelines for developing biotinylated diagnostics. Chem. Commun. 53, 2154–2157. https://doi.org/10.1039/C7CC00311K.

Jung, D., Maiti, S., Lee, J.H., Lee, J.H., Kim, J.S., 2014. Rational design of biotin−disulfide−coumarin conjugates: a cancer targeted thiol probe and bioimaging. Chem. Commun. 50, 3044–3047. https://doi.org/10.1039/C3CC49790A.

Lewis, D., 2021. COVID-19 rarely spreads through surfaces. So why are we still deep cleaning? Nature 590, 26–28. https://doi.org/10.1038/d41586-021-00251-4.

Li, K., Hou, J.-T., Yang, J., Yu, X.-Q., 2017. A tumor-specific and mitochondria-targeted fluorescent probe for real-time sensing of hypochlorite in living cells. Chem. Commun. 53, 5539–5541. https://doi.org/10.1039/C7CC01679D.

Maiti, S., Park, N., Han, J.H., Jeon, H.M., Lee, J.H., Bhuniya, S., Kang, C., Kim, J.S., 2013. Gemcitabine–coumarin–biotin conjugates: a target specific theranostic anticancer prodrug. J. Am. Chem. Soc. 135, 4567–4572. https://doi.org/10.1021/ja401350x.

Nabi, G., Wang, Y., Hao, Y., Khan, S., Wu, Y., Li, D., 2020. Massive use of disinfectants against COVID-19 poses potential risks to urban wildlife. Environ. Res. 188, 109916. https://doi.org/10.1016/j.envres.2020.109916.

Pan, B., Ren, H., Lv, X., Zhao, Y., Yu, B., He, Y., Ma, Y., Niu, C., Kong, J., Yu, F., Sun, W.B., Zhang, Y., Willard, B., Zheng, L., 2012. Hypochlorite-induced oxidative stress elevates the capability of HDL in promoting breast cancer metastasis. J. Transl. Med. 65. https://doi.org/10.1186/1479-5876-10-65.

Park, S.Y., Won, M., Kim, J.S., Lee, M.H., 2020. Ratiometric fluorescent probe for monitoring tyrosinase activity in melanosomes of melanoma cancer cells. Sens. Actuators B Chem. 319, 128306. https://doi.org/10.1016/j.snb.2020.128306.

Rayner, B.S., Zhang, Y., Brown, B.E., Reyes, L., Cogger, V.C., Hawkins, C.L., 2018. Role of hypochlorous acid (HOCl) and other inflammatory mediators in the induction of macrophage extracellular trap formation. Free Radical Bio. Med. 129, 25–34. https://doi.org/10.1016/j.freeradbiomed.2018.09.001.

Rafiee, A., Delgado-Saborit, J.M., Sly, P.D., Amiri, H., Mosalaei, S., Hoseini, M., 2022. Health consequences of disinfection against SARS-CoV-2: exploring oxidative stress damage using a biomonitoring approach. Sci. Total Environ. 2022, 152832. https://doi.org/10.1016/j.scitotenv.2021.152832.

Rong, X., Liu, C., Li, M., Zhu, H., Zhang, Y., Su, M., Wang, X., Li, X., Wang, K., Yu, M., Sheng, W., Zhu, B., 2021. An integrated fluorescent probe for ratiometric detection of glutathione in the golgi apparatus and activated organelle-targeted therapy. Anal. Chem. 93, 16105–16112. https://doi.org/10.1021/acs.analchem.1c03836.

Service, R.F., 2020. Does disinfecting surfaces really prevent the spread of coronavirus? Science https://doi.org/10.1126/science.abb7058.

Shu, W., Zang, S., Wang, C., Gao, M., Jing, J., Zhang, X., 2020. An endoplasmic reticulum-targeted ratiometric fluorescent probe for the sensing of hydrogen sulfide in living cells and zebrafish. Anal. Chem. 92, 9982–9988. https://doi.org/10.1021/acs.analchem.0c01623.

Said, H.M., 1999. Cellular uptake of biotin: mechanisms and regulation. J. Nutr. 129, 490S–493S. https://doi.org/10.1093/jn/129.2.490S.

She, Z.-P., Wang, W.-X., Mao, G.-J., Jiang, W.-L., Wang, Z.-Q., Li, Y., Li, C.-Y., 2021. A near-infrared fluorescent probe for accurately diagnosing cancer by sequential detection of cysteine and H^+. Chem. Commun. 57, 4811–4814. https://doi.org/10.1039/D1CC01228B.

Thakur, A.K., Sathyamurthy, R., Velraj, R., Lynch, I., Saidur, R., Pandey, A.K., Sharshir, S.W., Kabeel, A.E., Hwang, J.-Y., GaneshKumar, P., 2021. Secondary transmission of SARS-CoV-2 through wastewater: concerns and tactics for treatment to effectively control the

pandemic. J. Environ. Manag. 290, 112668. https://doi.org/10.1016/j.jenvman.2021.112668.
Vadlapudi, A.D., Vadlapatia, R.K., Mitra, A.K., 2012. Sodium dependent multivitamin transporter (SMVT): a potential target for drug delivery. Curr. Drug Targets 13, 994–1003. https://doi.org/10.2174/138945012800675650.
WHO, 2021. Coronavirus Disease (COVID-19) Pandemic. https://www.who.int/emergencies/diseases/novel-coronavirus-2019.
Wang, B., Yuan, F., Wang, S., Duan, R., Ren, W.X., Hou, J.-T., 2021. Detection of atherosclerosis-associated HOCl using a mitochondria-targeted fluorescent probe. Sens. Actuators B Chem. 348, 130695. https://doi.org/10.1016/j.snb.2021.130695.
Wang, L., Liu, J., Zhang, H., Guo, W., 2021. Discrimination between cancerous and normal cells/tissues enabled by a near-infrared fluorescent HClO probe. Sens. Actuators B Chem. 334, 129602. https://doi.org/10.1016/j.snb.2021.129602.
Wang, S., Zhu, B., Wang, B., Cao, X., Zhu, L., Hou, J.-T., Zeng, L., 2021. Revealing HOCl burst from endoplasmic reticulum in cisplatin-treated cells via a ratiometric fluorescent probe. Chin. Chem. Lett. 32, 1795–1798. https://doi.org/10.1016/j.cclet.2020.12.039.
Wu, L., Liu, J., Tian, X., Groleau, R.R., Bull, S.D., Li, P., Tang, B., James, T.D., 2021. Fluorescent probe for the imaging of superoxide and peroxynitrite during drug-induced liver injury. Chem. Sci. 12, 3921–3928. https://doi.org/10.1039/D0SC05937D.
Wu, X., Wang, R., Qi, S., Kwon, N., Han, J., Kim, H., Li, H., Yu, F., Yoon, J., 2021. Rational design of a highly selective near-infrared two-photon fluorogenic probe for imaging orthotopic hepatocellular carcinoma chemotherapy. Angew. Chem. Int. Ed. 60, 15418–15425. https://doi.org/10.1002/anie.202101190.
Wang, Y., Chen, L., 2021. Smart fluorescent probe strategy for precision targeting hypoxic tumor. J. Med. Chem. 64, 2967–2970. https://doi.org/10.1021/acs.jmedchem.1c00433.
Wen, Y., Zhang, W., Liu, T., Huo, F., Yin, C., 2017. Pinpoint diagnostic kit for heat stroke by monitoring lysosomal pH. Anal. Chem. 89, 11869–11874. https://doi.org/10.1021/acs.analchem.7b03612.
Xu, Q., Lee, K.-A., Lee, S., Lee, K.M., Lee, W.J., Yoon, J., 2013. A highly specific fluorescent probe for hypochlorous acid and its application in imaging microbe-induced HOCl production. J. Am. Chem. Soc. 135, 9944–9949. https://doi.org/10.1021/ja404649m.
Ye, M., Han, Y., Tang, J., Piao, Y., Liu, X., Zhou, Z., Gao, J., Rao, J., Shen, Y., 2017. A tumorspecific cascade amplification drug release nanoparticle for overcoming multidrug resistance in cancers. Adv. Mater. 29, 1702342. https://doi.org/10.1002/adma.201702342.
Yang, W., Cheng, Y., Xu, T., Wang, X., Wen, L., 2009. Targeting cancer cells with biotin–dendrimer conjugates. Eur. J. Med. Chem. 44, 862–868. https://doi.org/10.1016/j.ejmech.2008.04.021.
Zhang, H., Tang, W., Chen, Y., Yin, W., 2020. Disinfection threatens aquatic ecosystems. Science 368, 146–147. https://doi.org/10.1126/science.abb8905.
Zhu, B., Liu, W., Zhang, M., Wang, Y., Liu, C., Wang, Z., Duan, Q., Jia, P., 2018. A highly specific and ultrasensitive near-infrared fluorescent probe for imaging basal hypochlorite in the mitochondria of living cells. Biosens. Bioelectron. 107, 218–223. https://doi.org/10.1016/j.bios.2018.02.023.
Zhu, B., Li, P., Shu, W., Wang, X., Liu, C., Wang, Y., Wang, Z., Wang, Y., Tang, B., 2016. Highly specific and ultrasensitive two-photon fluorescence imaging of native HOCl in lysosomes and tissues based on thiocarbamate derivatives. Anal. Chem. 88, 12532–12538. https://doi.org/10.1021/acs.analchem.6b04392.
Zhu, H., Liu, C., Su, M., Rong, X., Zhang, Y., Wang, X., Wang, K., Li, X., Yu, Y., Zhang, X., Zhu, B., 2021. Recent advances in 4-hydroxy-1,8-naphthalimide-based small-molecule fluorescent probes. Coordin. Chem. Rev. 448, 214153. https://doi.org/10.1016/j.ccr.2021.214153.
Zhu, H., Fan, J., Wang, J., Mu, H., Peng, X., 2014. An “Enhanced PET”-based fluorescent probe with ultrasensitivity for imaging basal and elesclomol-induced HClO in cancer cells. J. Am. Chem. Soc. 136, 12820–12823. https://doi.org/10.1021/ja505988g.
Zhu, B., Gao, C., Zhao, Y., Liu, C., Li, Y., Wei, Q., Ma, Z., Du, B., Zhang, X., 2011. A 4-hydroxynaphthalimide-derived ratiometric fluorescent chemodosimeter for imaging palladium in living cells. Chem. Commun. 47, 8656–8658. https://doi.org/10.1039/C1CC13215F.
Zhou, Y., Li, P., Fan, N., Wang, X., Liu, X., Wu, L., Zhang, W., Zhang, W., Ma, C., Tang, B., 2019. In situ visualization of peroxisomal peroxynitrite in the livers of mice with acute liver injury induced by carbon tetrachloride using a new two-photon fluorescent probe. Chem. Commun. 55, 6767–6770. https://doi.org/10.1039/C9CC02483B.